1   **Linear response of east Greenland's tidewater glaciers to ocean/atmosphere warming**

2   **T.R. Cowton*[1], A.J. Sole[2], P.W. Nienow[3], D.A. Slater[4] and P. Christoffersen[5]**

3   *corresponding author

4   [1]School of Geography and Sustainable Development, University of St Andrews, KY16 9AL, UK

5   [2]Department of Geography, University of Sheffield, S10 2TN, UK

6   [3]School of Geosciences, University of Edinburgh, EH8 9XP, UK

7   [4]Scripps Institute of Oceanography, UC San Diego, La Jolla, CA 92093, USA

8   [5]Scott Polar Research Institute, University of Cambridge, CB2 1ER, UK

9   **Abstract**

10   Predicting the retreat of tidewater outlet glaciers forms a major obstacle to forecasting the rate of

11   mass loss from the Greenland Ice Sheet. This reflects the challenges of modelling the highly dynamic,

12   topographically complex and data poor environment of the glacier–fjord systems that link the ice

13   sheet to the ocean. To avoid these difficulties, we investigate the extent to which tidewater glacier

14   retreat can be explained by simple variables: air temperature, meltwater runoff, ocean temperature,

15   and two simple parameterisations of 'ocean/atmosphere' forcing based on the combined influence

16   of runoff and ocean temperature. Over a 20-year period at 10 large tidewater outlet glaciers along

17   the east coast of Greenland, we find that ocean/atmosphere forcing can explain up to 76 % of the

18   variability in terminus position at individual glaciers and 54 % of variation in terminus position across

19   all 10 glaciers. Our findings indicate that 1) the retreat of east Greenland's tidewater glaciers is best

20   explained as a product of both oceanic and atmospheric warming and 2) despite the complexity of

21   tidewater glacier behaviour, over multi-year time scales a significant proportion of terminus position

22   change can be explained as a simple function of this forcing. These findings thus demonstrate that

23   simple parameterisations can play an important role in predicting the response of the ice sheet to

24   future climate warming.

25   **Significance statement**

26   Mass loss from the Greenland Ice Sheet is expected to be a major contributor to 21st Century sea

27   level rise, but projections retain substantial uncertainty due to the challenges of modelling the

28   retreat of the tidewater outlet glaciers that drain from the ice sheet into the ocean. Despite the

29   complexity of these glacier-fjord systems, we find that over a 20-year period much of the observed

30   tidewater glacier retreat can be explained as a predictable response to combined atmospheric and

31   oceanic warming, bringing us closer to incorporating these effects into the ice sheet models used to

32   predict sea level rise.

Introduction

Loss of mass from tidewater glaciers to the ocean through iceberg calving and submarine melting is a major component of the mass budget of the Greenland Ice Sheet (GrIS). The contribution of this *frontal ablation* to ice sheet mass balance can vary dramatically on short timescales: increased frontal ablation was responsible for 39 % of GrIS mass loss from 1991-2015 (van den Broeke et al., 2017), and accounted for as much as two thirds of GrIS mass loss during a phase of rapid retreat, acceleration and thinning of outlet glaciers between 2000-05 (Rignot and Kanagaratnam, 2006). Understanding the controls on frontal ablation is thus crucial if its contribution to the mass budget of the GrIS is to be predicted by models (e.g. Nick et al., 2013).

Frontal ablation and tidewater glacier retreat are closely interlinked – if ice loss at the terminus is more rapid than the delivery of ice from up-glacier, the terminus will retreat. A leading hypothesis attributes the recent rapid retreat of many of Greenland's tidewater glaciers to an increase in submarine melting, and consequently calving, in response to oceanic warming (e.g. Straneo and Heimbach, 2013). Alternatively, retreat may have been driven by increasing surface melt, with meltwater runoff draining through glaciers and entering fjords at depth to form buoyant plumes which enhance submarine melting at glacier termini (e.g. Jenkins, 2011, Fried et al., 2015). It has also been suggested that increased surface melt and runoff may accelerate calving through hydrofracturing of near-terminus crevasses (e.g. Nick et al., 2013), or by increasing basal water pressure and hence basal motion (e.g. Sugiyama et al., 2011). A third hypothesis links retreat to increased calving rates following a reduction in terminus buttressing by ice mélange and land-fast sea ice (e.g. Christoffersen et al., 2012, Moon et al., 2015). In most cases however, it has not proven possible to attribute observed variability in terminus position to a particular cause, especially when multiple glaciers are considered (e.g. McFadden et al., 2011, Bevan et al., 2012, Carr et al., 2013, Moon et al., 2015, Murray et al., 2015).

The lack of a clear relationship between observed tidewater glacier retreat and changing environmental conditions presents a significant issue for modelling studies which seek to predict mass loss from the GrIS under a warming climate (e.g. Goelzer et al., 2013, Fürst et al., 2015). One challenge in establishing a causal relationship between environmental forcings and tidewater glacier retreat is that at the scale of individual glaciers these relationships often appear highly nonlinear, with feedbacks triggered as the terminus retreats across uneven bed topography obscuring the forcing driving the initial retreat (e.g. Vieli et al., 2002). This difficulty is compounded by a poor understanding of the oceanic forcing of these glaciers, due both to the scarcity of observations and the complexities of calving and submarine melt processes at glacier termini (Straneo et al., 2013). A

66   further issue is that accurately representing these processes in ice sheet and ocean models would

67   require model resolution and a knowledge of boundary conditions that lies beyond current

68   capabilities (Benn et al., 2017).

69   In this paper, we seek to address these challenges to improve our understanding of the retreat of

70   Greenland's tidewater glaciers on timescales relevant to predictions of mass loss over coming

71   decades. We focus our study on 10 tidewater glaciers along Greenland's east coast of varying size

72   and spanning > 10° of latitude (Table S1; Figure 1). Over a 20-year period (1993-2012) we compare

73   the observed pattern and rate of retreat with variability in five environmental forcings, assessing the

74   ability of these forcings to explain variability in the terminus position (P) of the study glaciers, both

75   individually and collectively. These forcings comprise near-terminus air temperature (T_A), glacier

76   meltwater runoff (Q), ocean temperature (T_O) and two parameterisations of combined

77   'ocean/atmosphere' forcing (M_1 and M_2). These ocean/atmosphere forcing parameterisations reflect

78   the theory that frontal ablation will depend not only on ocean temperature but also runoff due to its

79   role in stimulating buoyant upwelling adjacent to the terminus (e.g. Jenkins, 2011, Chauché et al.,

80   2014) and driving the renewal of warm water in the fjord (e.g. Cowton et al., 2016, Carroll et al.,

81   2017), thereby increasing the transfer of heat between the ocean and ice. To represent this

82   combined ocean/atmosphere forcing we define $M_1 = Q(T_O\text{-}T_f)$ and $M_2 = Q^{1/3}(T_O\text{-}T_f)$. In these

83   parameterisations, ocean temperature is expressed relative to the *in situ* freezing point at the

84   calving front, approximated as T_f = -2.13 °C based on a depth of 300 m and salinity of 34.5 psu (e.g.

85   Straneo et al., 2012). M_1 is thus a simple product of runoff and the oceanic heat available for

86   melting, while the addition of the exponent to the formulation for M_2 is based on the expectation

87   that submarine melt rate will scale linearly with temperature and with runoff raised to the power of

88   1/3 (Jenkins, 2011).

89   **Results**

90   Time series of variability in T_A, Q, T_O and P for each of the study glaciers are plotted in Figure 2 (see

91   also Methods). These time series, along with the two ocean/atmosphere forcings M_1 and M_2, are

92   displayed as normalised values for each glacier in Figure 3. Glaciers are grouped into 'northern' and

93   'southern' subsets based on their location with respect to a steep latitudinal gradient in ocean

94   temperature at ~69° N, which reflects the influence of the Irminger Current (Seale et al., 2011;

95   Figure 1). Features specific to the individual glaciers (in particular, fjord and subglacial topography)

96   may modify their response to environmental forcings (e.g. Carr et al., 2013), and so the normalised

97   values are also averaged for the five southern and five northern glaciers to show the regional trends,

98   thereby emphasising the climatic signal (Figure 3f,l).

99   We begin by examining the relationship between terminus position and the environmental forcings

100   at the scale of individual glaciers. At the southern glaciers, there is a marked increase in the values of

101   the forcings and retreat of the glaciers between 2000 and 2005, with periods of relative stability

102   either side (Figures 2 and 3a-f). There are strong correlations between P and the forcings (R^2 = 0.24-

103   0.76, depending on the glacier and forcing; Figure 4, Table S2) for both the individual glaciers and

104   regional trends. Because the time series involved are non-stationary, there is however an increased

105   risk of spurious correlations resulting from similar long-term trends in the forcing and response

106   variables existing over the study period (Granger and Newbold, 1974). We therefore run an Engle-

107   Granger test for cointegration (Engle and Granger, 1987), which facilitates statistical comparison

108   between two (or more) non-stationary time series showing stochastic trends (Methods). We find

109   that P is significantly cointegrated ($p < 0.05$) with Q and M_1 at all of the southern study glaciers, with

110   T_A and T_O at Mogens 3 (M3), AP Bernstorffs Glacier (AB) and Helheim Glacier (HG), and with M_2 at AB

111   and HG (Figure 4, Table S2). Cointegration indicates a temporally-constant functional relationship,

112   meaning that these results support the existence of causal relationships between P and the

113   environmental forcings. However, because the forcings demonstrate similar temporal variability to

114   each other, determining which (if any) is the key control on terminus position from this analysis

115   alone remains difficult.

116   The results are qualitatively similar at the northern glaciers, which show a brief retreat during a

117   phase of higher T_A, Q and T_O (and thus also M_1 and M_2) between ~1994-1995, then a slight re-

118   advance, before embarking on a more sustained retreat in keeping with the increase in the forcings

119   after ~2001 (Figure 3g-l). The statistical significance of these trends is however weaker at the

120   northern glaciers (Figure 4 and Table S2), with significant cointegration of P with all forcings at

121   Daugaard-Jensen Glacier (DJ) and with M_1 and M_2 at Waltershausen Glacier (WG). This may be due

122   in part to the smaller absolute variability in the time series at the northern glaciers, increasing the

123   magnitude of short-term noise relative to the long-term trends (Figures 2 and 3). Nevertheless, clear

124   similarities appear between the variability in the forcings in P when the normalised data from the

125   northern glaciers are combined to show the regional trends (Figure 3l). Correlation of the individual

126   forcings and P for the combined northern glaciers data sets give R^2 values of 0.51-0.63 (significant at

127   $p < 0.01$, Figure 4, Table S2); however, only M_1 is significantly cointegrated with P at $p < 0.05$.

128   This analysis indicates that, despite the complexities introduced by bed topography and ice

129   dynamics, over timescales of a few years or more many individual glaciers display a largely linear

130   response to environmental forcings. This is particularly apparent at the southern glaciers, where

131   both the increase in forcings and glacier retreat have been more pronounced (Figures 2 and 3).

132   However, because at this level P demonstrates strong correlations with multiple forcings, it remains

133   unclear whether this retreat has been driven primarily by warming of the atmosphere, ocean, or

134   both. To gain further insight, we therefore examine variation in glacier retreat across all 10 study

135   glaciers.

136   Any environmental control on P should also be able to explain variation in retreat rate between

137   glaciers. In particular, the absolute magnitude of retreat is consistently lower at the northern

138   compared to the southern glaciers (with the standard deviation in P at the northern glaciers just 17

139   % of that exhibited at the southern glaciers), a trend which remains true for an expanded sample of

140   32 of east Greenland's tidewater glaciers (Seale et al., 2011). When the absolute variability at all

141   glaciers is considered together, there is a significant ($p < 0.01$) correlation of P with Q (Figure 5a; $R^2 =$

142   0.40), T_O (Figure 5b; $R^2 = 0.36$) and T_A (Figure 5a; $R^2 = 0.21$). However, while T_A, Q and T_O are all

143   typically higher at the southern than the northern glaciers, the latitudinal difference in the

144   magnitude of the variability is less marked compared to that in P: the standard deviation in Q, T_O and

145   T_A at the northern glaciers is 60, 74 and 93 % respectively of the standard deviation at the southern

146   glaciers. The implication is that for a given change in these forcings, the southern glaciers have

147   responded more sensitively than the northern glaciers. Combining Q and T to create M_1 and M_2

148   increases the latitudinal gradient in the forcings to give better agreement with that observed in P,

149   with the standard deviation in both M_1 and M_2 at the northern glaciers 36 % of that exhibited at the

150   southern glaciers. Combined with a good correlation at the glacier level (Figure 4), this helps to

151   strengthen the correlation *of P with M_1* (Figure 5c; $R^2 = 0.54$), and to a lesser extent the slightly more

152   complex ocean/atmosphere forcing parameter M_2 (Figure 5d; $R^2 = 0.45$).

153   We additionally test the ability of the environmental forcings to explain only the inter-glacier

154   variability in long-term retreat rate, a property of arguably greater importance than the year-to-year

155   variability from the perspective of predicting future ice sheet mass loss. To examine this, we

156   compare the overall retreat of each glacier (defined as the difference between the mean values from

157   1993-1995 and 2010-2012) against the equivalent change in the five forcings. Again M_1 and M_2

158   provide the strongest correlation, giving R^2 values of 0.54 and 0.57 ($p < 0.01$) respectively, compared

159   to 0.41 ($p < 0.01$) for T_O (Figure 5e-h; Table S3). There is no significant correlation between the

160   magnitude of the overall change in P and T_A and Q at $p < 0.05$, with the northern glaciers again

161   showing a much smaller retreat for a given increase in the atmospheric forcing.

162   **Discussion**

163   Our findings demonstrate that the timing and magnitude of tidewater glacier retreat along

164   Greenland's east coast can be effectively explained as a combined linear response to atmospheric

165   and oceanic conditions. Whilst variation in runoff alone can explain a large proportion of glacier

166   retreat at individual glaciers (Figure 4), the sensitivity of this relationship is much stronger in

167   southeast Greenland where ocean waters are warmer (and continued to warm more rapidly over

168   the study period) compared to northeast Greenland (Figure 5a-b,f-g). It may thus be that contact

169   with warm ocean waters preconditions the southern glaciers to greater sensitivity to changes in

170   atmospheric temperature and hence runoff – if the ocean temperature is close to the *in situ* melting

171   point, this will limit the potential for submarine melting, irrespective of the vigour of runoff-driven

172   circulation. Whilst previous studies have hypothesised that regional differences in glacier stability in

173   east Greenland may be linked to the strong latitudinal ocean temperature gradient (Seale et al.,

174   2011, Walsh et al., 2012) and that a combined warming of ocean and atmosphere may provide the

175   key trigger for rapid glacier retreat (Bevan et al., 2012, Christoffersen et al., 2012), we are able to

176   demonstrate quantitatively that the combined influence of ocean and atmospheric temperature

177   provides the strongest predictor of both spatial and temporal variation in glacier terminus position

178   (Figure 5). In this way, our results agree with recent observations from the Antarctic Peninsula which

179   show that, while there has been a strong atmospheric warming trend in this region, the magnitude

180   of glacier retreat is much greater in areas where glaciers are in contact with warm Circumpolar Deep

181   Water (Cook et al., 2016). While the existence of a correlation cannot alone provide conclusive

182   evidence of a causal link, our results thus join a growing body of evidence indicating a role for both

183   oceanic and atmospheric warming in driving the retreat of marine-terminating outlet glaciers.

184   Our results suggest that variability in terminus position across the 10 study glaciers can be

185   parameterised as

186
$$\frac{dP}{dt} = a\frac{dM_1}{dt},$$

187   (1)

188   where t is time and a = -0.014±0.002 or -0.018±0.006 km / (m^3 s^{-1} °C) depending on whether the

189   parameterisation is fitted to maximise agreement with the year-to-year variability (Figure 5d) or

190   overall retreat (Figure 5i) respectively (Figure S3). This simple formulation effectively captures both

191   the temporal variability in the rate of change of glacier front position and the widely differing

192   magnitude of response at the different outlet glaciers (Figure 6). Across 10 glaciers, equation (1) can

193   explain 54 % of year-to-year variability in terminus position (Figure 5d) and 54 % of variation in the

194   overall retreat rate (Figure 5i). As such, while the prediction of individual tidewater glacier behaviour

195   on timescales of a few years or less may require detailed glacier-specific knowledge of bedrock

196   topography (e.g. Howat et al., 2008, Carr et al., 2013) and high-resolution modelling of ice dynamics

197   (e.g. Todd et al., 2018), our results show that on longer timescales variation in the glaciers' terminus

198   positions can be captured with much simpler parameterisations. These parameterisations translate

199   the complex interaction of ice sheets with the atmosphere and ocean into simple yet statistically

200   strong relationships that provide a new pathway for the inclusion of tidewater glacier retreat in the

201   large-scale ice sheet models needed to predict global sea level rise (e.g. Fürst et al., 2015,

202   Aschwanden et al., 2016).

203   This quasi-linear behaviour likely reflects the complex topography and thus relatively frequent

204   occurrence of pinning points (such as lateral constrictions and submarine sills) within Greenlandic

205   glacier-fjord systems. This means that, unlike regions of West Antarctica where bed topography may

206   precondition the ice sheet to centennial scale unstable retreat (e.g. Joughin et al., 2014), change at

207   many of Greenland's tidewater glaciers may occur as series of rapid short-lived retreats which

208   collectively do not deviate far from the linear response to climate warming. Capturing the exact

209   timing and magnitude of these steps is difficult and may not be necessary if the aim is to predict ice

210   sheet mass loss on timescales of decades or longer. A good example of this can be seen when

211   comparing KG and Helheim Glacier (HG): as the forcings increased between 2000 and 2005, HG

212   retreated steadily whilst KG remained comparatively stable before undergoing a rapid ~ 5 km retreat

213   between topographic pinning points in 2004-5 (Figures 3d-e and S1). If viewed over the period 2000

214   to 2005, the retreat of KG appears sudden while the retreat of HG appears prolonged; however,

215   when considered over the full 20-year time series, both glaciers exhibited a broadly similar retreat

216   between 2000-2005 with periods of comparative stability before and after.

217   This topographic influence accounts for some of the largest outliers in the relationship between P

218   and M_1 (Figure 5d), with a ~3-4 km discrepancy between the observed and parameterised modelled

219   terminus position briefly existing at KG due to the delayed response of this glacier to

220   ocean/atmosphere warming during 2000-2005 (Figures 3e and 6a). At KG, this discrepancy is short-

221   lived, but this observation illustrates how equation (1) is likely to be least effective at glaciers at

222   which current behaviour is particularly strongly influenced by topography: for example, looking to

223   west Greenland, Jakobshavn Isbræ may have been undergoing an unstable retreat into deeper water

224   since the loss of its floating tongue in the late 1990s (Joughin et al., 2008), whilst the stability of

225   Store Glacier to the north is attributed to the presence of an exceptionally prominent topographic

226   pinning point (Todd et al., 2018). While such glaciers will ultimately adjust to a new climatically

227   stable position, their terminus position may differ more strongly from the linear trend in the short

228   term. Nevertheless, our findings suggest that simple formulations such as equation (1) can play an

229   important role in parameterising the response to climate warming of many tidewater glaciers,

230   including major outlets such as KG, HG and DJ.

231   The efficacy of this approach is likely to be dependent on the timeframe in question. The influence

232   of topographic pinning points will be magnified on short timescales (~5 years or less), with this effect

233   reduced when retreat rates are averaged over longer timescales. Furthermore, the slow response

234   time of glaciers will modulate climatic signals by filtering out higher frequency variation – for

235   example, this may explain the muted response of the southern glaciers to the short-lived

236   cooling/warming over 2009-10 (Figure 2-3). At much longer timescales, glaciers will become less

237   sensitive to the ocean as they retreat into shallower water and onto dry land, while evolving ice

238   sheet mass balance and geometry will also likely impact upon the relationship between forcings and

239   terminus position. We therefore suggest that the relationship described in equation (1) is most

240   appropriate when considering processes on timescales of ~5-100 years, with uncertainty increasing

241   either side of this window.

242   The dependency of retreat rate on both runoff and ocean temperature points to a key role for

243   calving front processes in driving the retreat of Greenland's tidewater glaciers. The obvious link lies

244   in submarine melting: theory and modelling suggest that submarine melt rate is dependent on both

245   ocean temperature and runoff, with the latter driving buoyant plumes that increase the turbulent

246   transfer of oceanic heat to glacier calving fronts (e.g. Jenkins, 2011, Xu et al., 2013). The role of

247   submarine melting as a control on terminus position appears straightforward where glaciers are

248   relatively slow flowing and warm ocean waters are capable of inducing submarine melt rates on par

249   with ice velocity; in such circumstances undercutting by submarine melting may be the primary

250   source of frontal ablation (Bartholomaus et al., 2013, Luckman et al., 2015), such that changes in

251   terminus position are determined by the difference between ice velocity and submarine melt rate

252   (Slater et al., 2017). The applicability of this mechanism at faster flowing glaciers is less clear

253   however, as predictions of ice front-averaged submarine melt rates fall far below terminus velocities

254   (Todd and Christoffersen, 2014, Rignot et al., 2016). Indeed, observations indicate a mechanistic

255   difference between the small scale calving in submarine melt dominated systems (Luckman et al.,

256   2015) and the massive buoyant calving of icebergs from Greenland's largest and fastest flowing

257   glaciers (James et al., 2014). Nevertheless, our findings indicate that terminus position at these large

258   and fast flowing glaciers also responds rapidly and predictably to variability in ocean/atmosphere

259   forcing.

260   We also note that the lack of improvement in the correlation between P and M_2 (= $Q^{1/3}(T_O-T_f)$)

261   compared to M_1 (= $Q(T_O-T_f)$) is at odds with the dependency expected if retreat rate was a direct

262   function of submarine melt rate (Jenkins, 2011). It may be that this theoretical relationship (which is

263   yet to be validated by field data) does not reflect the reality of the relationship between T_O, Q and

264   submarine melting - for example, Slater *et al* (2016) report that the correct value for the exponent

265   may be as high as ¾ under certain circumstances. Alternatively, the apparently simple relationship

266   between P and M_1 may be the integrated result of not only submarine melting but also additional

267   factors including ice mélange / sea ice coverage (e.g. Christoffersen et al., 2012, Moon et al., 2015)

268   and hydrologically forced acceleration of ice motion (e.g. Sugiyama et al., 2011). The stronger

269   correlations between P and Q rather than T_A (Figures 4 and 5) indicate that catchment-wide melt,

270   and hence runoff, is of greater importance than local air temperatures at the terminus as a control

271   on retreat rate. While this suggests that processes driven by local surface melting (e.g. through

272   hydrofracture-driven calving) are of secondary importance, we cannot discount the possibility that

273   our results reflect a more complex mix of processes related to basal hydrology, glacier dynamics,

274   submarine melting and calving. Thus whilst our findings indicate that a combined ocean/atmosphere

275   forcing is a key control on the stability of even large, fast flowing tidewater glaciers, further research

276   is needed to identify and constrain the processes that link this forcing with frontal ablation and

277   glacier retreat.

278   Over a 20-year period, we have observed a significant correlation between variability in glacier

279   terminus position and a simple parameterisation that combines oceanic and atmospheric forcings at

280   10 tidewater glaciers along Greenland's east coast. Our results demonstrate that while increased

281   melting and runoff in response to atmospheric warming can explain much of the temporal variability

282   in glacier terminus position, the temperature of the adjacent ocean waters is also a strong

283   determinant of the absolute magnitude of retreat. We find that even at very large and fast flowing

284   glaciers like Kangerdlugssuaq Glacier and Helheim Glacier, where the nonlinear response to climate

285   forcing has previously been emphasised, over timescales of a few years or longer, this forcing

286   dominates over site-specific effects relating to the complexities of local topography. While

287   topography remains an important factor in modulating the response of tidewater glaciers to climate,

288   our findings nevertheless suggest that simple parameterisations linking terminus retreat to runoff

289   and ocean temperature, suitable for inclusion in large-scale ice sheet models, have an important role

290   to play in modelling the response of the Greenland ice sheet to atmospheric and oceanic warming.

291

292   **Methods**

293   *Study glaciers*

294   Details of the 10 study glaciers are given in Table S1. These glaciers represent a subset of the 32

295   glaciers documented by Seale *et al* (2011), chosen to span a range of conditions along the east coast

296   of Greenland. Within each region, the largest outlet glaciers (with respect to ice velocity and

297   terminus width; Table S1) were selected. In the far northeast of Greenland, the major outlet glaciers

298   drain into substantial floating ice tongues (e.g. Wilson et al., 2017). Charting the retreat of these

299   glaciers (where changes in grounding line position rather than calving front position are likely of

300   primary importance) is not possible with the methods employed here, and so no glaciers were

301   selected in this region.

302   *Air temperature*

303   Mean summer air temperature (Figure 2a-b), T_A, is based on the May-September mean of monthly

304   temperatures from ERA-Interim global atmospheric reanalysis (Dee et al., 2011). For each glacier,

305   temperatures are extracted from the reanalysis cell in which the terminus lies. To account for

306   differing mean topography between cells, these values are adjusted to give sea level temperature

307   assuming an atmospheric lapse rate of 0.0065 °C / m.

308   *Runoff*

309   Annual mean catchment runoff, Q, for each of the 10 glaciers (Figures 1 and 2c-d) is obtained from a

310   1 km surface melting, retention and runoff model forced with ERA-Interim and 20CR reanalyses

311   (Wilton et al., 2017). Runoff due to basal melting is expected to be limited and is therefore not

312   considered. Meltwater is routed through glacial catchments using the hydraulic potential gradient

313   (Shreve, 1972) based on the ice surface and bed topography (Bamber et al., 2013). Q is predicted to

314   be greatest at KG due to its large catchment area and more melt-favourable hypsometry relative to

315   HG and DJ, which have comparable catchment areas (Figures 1 and 2c-d).

316   *Ocean temperature*

317   We seek to compare changes in glacier terminus position to a measure of ocean water temperature,

318   T_O, in the fjords adjacent to the glaciers. Because there are few *in situ* hydrographic measurements

319   from fjords, and the fjords are not well resolved in ocean circulation models, we define $T_O = T_R + c$,

320   where T_R is ocean temperature based on reanalysis values for the continental shelf and c is a

321   correction to account for temperature differences between the shelf and fjords.

322   T_R is obtained from the GLORYS2V3 1/4° ocean reanalysis product (Ferry et al., 2012). A decision

323   must be made as to where to sample these data for each glacier. Because cross-shelf troughs are

324   poorly mapped and not well resolved in the reanalysis, cells close to fjord mouths tend to be

325   unrealistically shallow (e.g. Fenty et al., 2016) and so the warmer, deeper waters (crucial to the fjord

326   heat budget) are not captured. Conversely, if the nearest cell of depth equal to that of the grounding

327   line is chosen, this can be hundreds of kilometres away from the fjord mouth on the shelf break, and

328   it is not clear that a pathway of such depth will exist between that cell and the glacier. As a

329   compromise, we opt for the nearest cell of depth > 400 m, which is deep enough to sample the

330   warmer Atlantic waters (AW) existing at depths greater than ~ 200 m whilst in many cases being

331   located on the shelf rather than beyond the shelf break (Figure 1). For simplicity and consistency

332   between glaciers, we take T_R as the annual mean temperature between 200-400 m (Figure 2e-f). This

333   falls within the likely depth range of up-fjord currents (e.g. Cowton et al., 2016), and allows key

334   inter-annual trends in AW temperature to be captured whilst reducing noise due to large seasonal

335   variations in shelf surface water temperatures which likely have limited influence on the glaciers

336   (Straneo and Heimbach, 2013).

337   To obtain values for the correction term c, we test these time series of T_R against available *in situ*

338   observations from moorings and CTD surveys in the vicinity of T1 (Holfort et al., 2008, Murray et al.,

339   2010), HG (Straneo et al., 2016), KG (Azetsu-Scott and Syvitski, 1999, Dowdeswell, 2004, Straneo et

340   al., 2012, Inall et al., 2014) and, in the absence of data from the northern study glaciers,

341   Nioghalvfjerdsbræ (NG) in the far north east of Greenland (Wilson and Straneo, 2015) (Figures 1 and

342   S2). Fitting of T_R to the observations indicates that the reanalysis data overestimate *in situ*

343   temperatures in these locations by approximately 1.5 °C (T1), 2.9 °C (HG), 3.1 °C (KG) and 0.3 °C

344   (NG). While this may in part reflect errors in the reanalysis product (which is poorly constrained by

345   observations on the shelf), significant cooling of AW is expected as it crosses the continental shelf

346   from the core of the warm currents at the shelf break to the fjords (Straneo et al., 2012). To better

347   represent the temperature of subsurface waters entering the fjords, we use these observations to

348   adjust the values of T_R derived from the reanalysis data to give T_O. For the cluster of glaciers in

349   southeast Greenland (M3, T1 and AB) we set c = 1.5 °C, while at HG and KG we set c = 2.9 °C and 3.1

350   °C respectively. For the glaciers in northeast Greenland (BG, VG, DJ, WG, HK), influenced by the same

351   cooler recirculated AW as NG (Straneo et al., 2012), we set c = 0.3 °C. These offsets are then used to

352   calculate the values of T_O used throughout the paper. While this adjustment is necessarily

353   approximate given the scarcity of *in situ* observations, its application enables better representation

354   of the temporal and spatial variability in the temperature of ocean water entering Greenland's

355   fjords.

356   *Terminus position*

357   For the period 2000-2009, width-averaged changes in glacier terminus position P (expressed as

358   distance from an arbitrary up-glacier location) are taken from Seale *et al* (2011) and based on the

359   automated classification of all available MODIS imagery. We extend this time series by manual

360   termini delineation (using the linear box method (Lea et al., 2014)) in Landsat scenes (e.g. Figure S1)

361   at approximately monthly intervals over the period 2009-2015, and where available over the period

362   1990-1999. No Landsat scenes are available during the years 1991, 1993 and 1995. At KG, HG and DJ

363   we supplement these data with terminus positions delimited using Envisat imagery by Bevan *et al*

364   (2012).

365   Because the glaciers typically undergo an annual cycle of advance and retreat, error will be

366   introduced into the mean annual position for glaciers and years where there are significant gaps in

367   the available coverage. We therefore adjust glacier lengths according to

$$P = P_{mean} + \left(\frac{1}{2}\mu_a r\right),$$

368   (2)

369   where P is the adjusted mean annual terminus position, as based on P_{mean}, which is the mean of the

370   available data for each year. r is the typical annual range in terminus positions for each glacier, based

371   on the period 2010-2013 when continuous Landsat availability gives accurate near year-round

372   coverage (Table S4). Each data point is given a weighting μ based on the month within which it falls,

373   ranging linearly from 1 (October, when the termini are typically most retreated), to -1 (April, when

374   the termini are typically most advanced). The mean weighting for each year, μ_a, thus provides an

375   indication of the extent by which the available data points likely over or under estimate the true

376   mean annual terminus position. For example, the only two data points for 1995 at DJ fall in August

377   and September (when the glacier length will be close to its annual minimum). This gives $\mu_a = 0.5$, and

378   P is thus increased by 0.25 x r (= 0.3 km) with respect to P_{mean} to better approximate the true annual

379   average terminus position. The difference between P_{mean} and P is shown in Figure 3 (being too small

380   to plot in Figure 2g-h) and is in most cases negligible.

381   *Statistics*

382   Statistical comparison of T_A, Q, T_O, M_1 and M_2 with P is undertaken at the level of mean annual

383   values. In Figure 5 (and Table S3) we consider data grouped from across the study glaciers, while in

384   Figures 3 and 4 (and Table S2) we relate individual glacier-specific time series of anomalies in T_A, Q,

385   T_O, M_1 and M_2 to those in P. Because these individual time series are in general non-stationary,

386   classical linear regression may indicate a statistically significant correlation between variables in

387   instances where in fact no relationship exists (Granger and Newbold, 1974). To reduce the risk of

388   incorrectly interpreting such spurious relationships, we test for cointegration of the time series

389   (Engle and Granger, 1987), a technique that has proven valuable in examining the relationships

390   between non-stationary climate variables (e.g. Kaufmann and Stern, 2002, Mills, 2009, Beenstock et

391   al., 2012). Cointegration occurs when a relationship between two or more non-stationary time series

392   produces residuals that are themselves stationary, indicating a functional relationship that remains

393   constant in time. A more thorough description of this approach, and its application in climate

394   science, is provided by Kaufman and Stern (2002). We perform an Engle-Granger test for

395   cointegration on each of the combinations of forcing and response time series using the *egcitest*

396   function in Matlab R2016a (www.mathworks.com). Where linear regression indicates a significant

397   correlation but cointegration is not established (at $p < 0.05$), we recognise the increased risk that this

398   correlation may be spurious. All R^2 values given throughout the paper are significant at $p < 0.05$, with

399   the specific p value given in each case, and all statistical values provided in Tables S2-3.

400

408   **Figures**

409
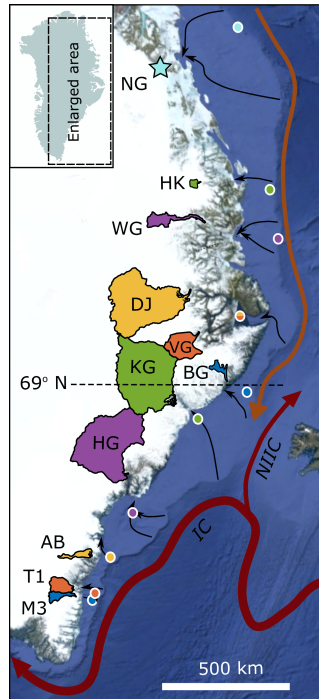
410

411

412 Figure 1. Map showing the location of the ten study glaciers (Table S1) in east Greenland: M3 =
413 Mogens 3; T1 = Tingmjarmiut 1; AB = AP Bernstorffs Glacier; HG = Helheim Glacier; KG =
414 Kangerdlugssuaq Glacier; BG = Borggraven; VG = Vestfjord Glacier; DJ = Daugaard-Jensen Glacier;
415 WG = Waltershausen Glacier; HK = Heinkel Glacier. The location of Nioghalvfjerdsbræ (NG), which is
416 referenced but does not constitute one of the study glaciers, is marked with a star. Hydrological
417 catchments are shaded, and the divide between the northern and southern study glaciers at ~69° N
418 is marked with the dashed line. The sample locations for ocean reanalysis temperature for the
419 glaciers are shown as coloured circles. Also shown are the approximate locations of warm ocean
420 currents (Straneo et al., 2012), with IC = Irminger Current and NIIC = North Iceland Irminger Current,
421 and cross shelf troughs that may allow warm subsurface waters to access the study glaciers (black
422 arrows; Jakobsson et al., 2012). The background image shows a satellite mosaic of Greenland with
423 shaded sea floor bathymetry (Google Earth; Data: SIO, NOAA, U.S. Navy, NGA, GEBCO; Image:
424 Landsat / Copernicus, IBCAO, U.S. Geological Survey).

425

426

427

428
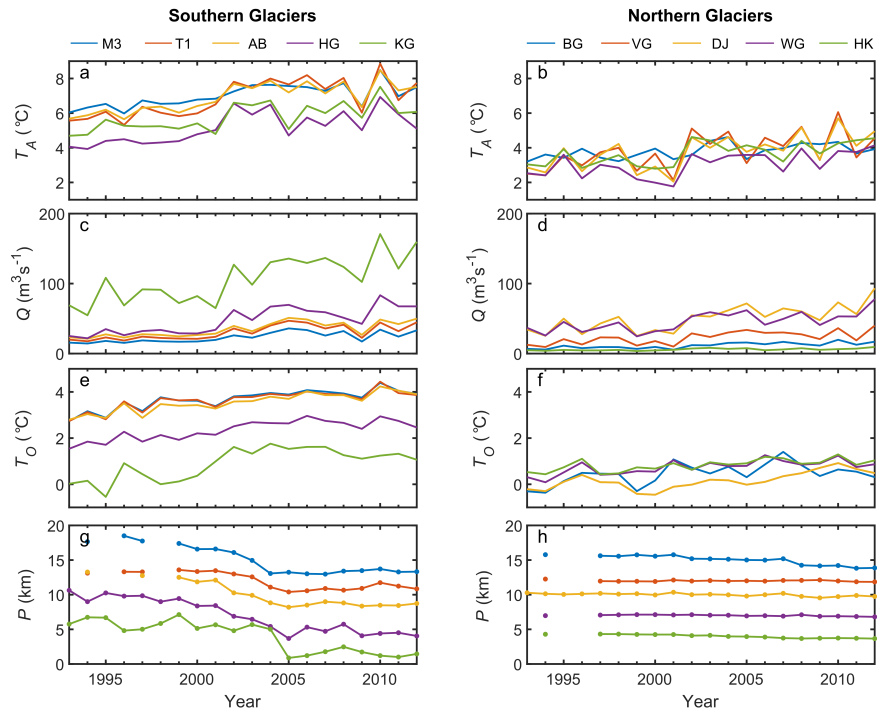
Figure 2. Annual average values of (a-b) air temperature (T_A), (c-d) runoff (Q), (e-f) depth-averaged subsurface ocean temperature (T_O) and (g-h) glacier terminus position (P), relative to an arbitrary up-glacier location, for the 10 study glaciers (Methods; Table S1). The left and right columns show glaciers south and north of ~69N respectively, and colours are as for Figure 1.

433

434

435
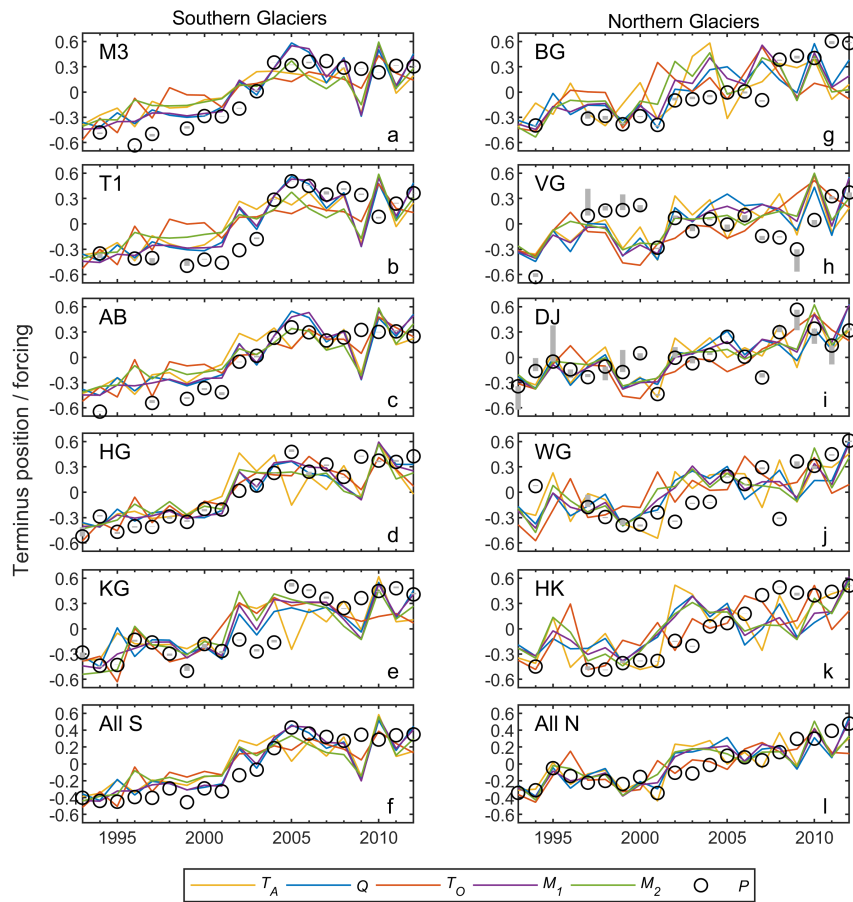
Figure 3. Time series of normalised anomalies in air temperature ($\tilde{T}_A$, orange) runoff ($\tilde{Q}$, blue), ocean temperature ($\tilde{T}_O$, red), $\tilde{M}_1$ (purple) and $\tilde{M}_2$ (green) and terminus position ($\tilde{P}$, black circles) for each glacier. Anomalies are expressed relative to the 20-year mean, and all values are normalised with respect to the observed range at that glacier. For ease of comparison, $\tilde{P}$ is shown inverted (i.e. positive change means retreat) and is in some cases discontinuous due to lack of observations. Vertical grey bars indicate the adjustment of P relative to P_{mean} (Methods).

442

443
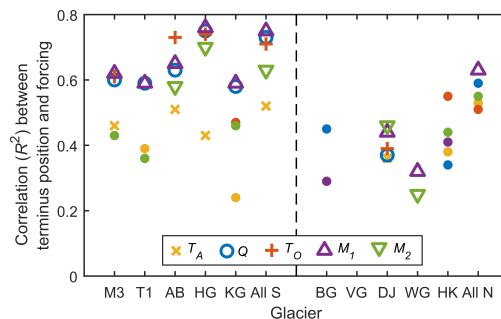
Figure 4. R^2 values for the relationship of terminus position (P) with air temperature (T_A) runoff (Q), ocean temperature (T_O) and M_1 and M_2 at each glacier and for the averaged regional southern ('All S') and northern ('All N') trends (Figure 3). Large markers show time series that are significantly

cointegrated at $p < 0.05$. Solid dots show instances which are correlated at $p < 0.05$, but are not
448 cointegrated at this confidence level. No marker is shown where the time series are not significantly
449 correlated or cointegrated. The dashed line separates the southern (left) and northern (right) glacier
450 subsets. Statistical values are given in Table S2.

451

452
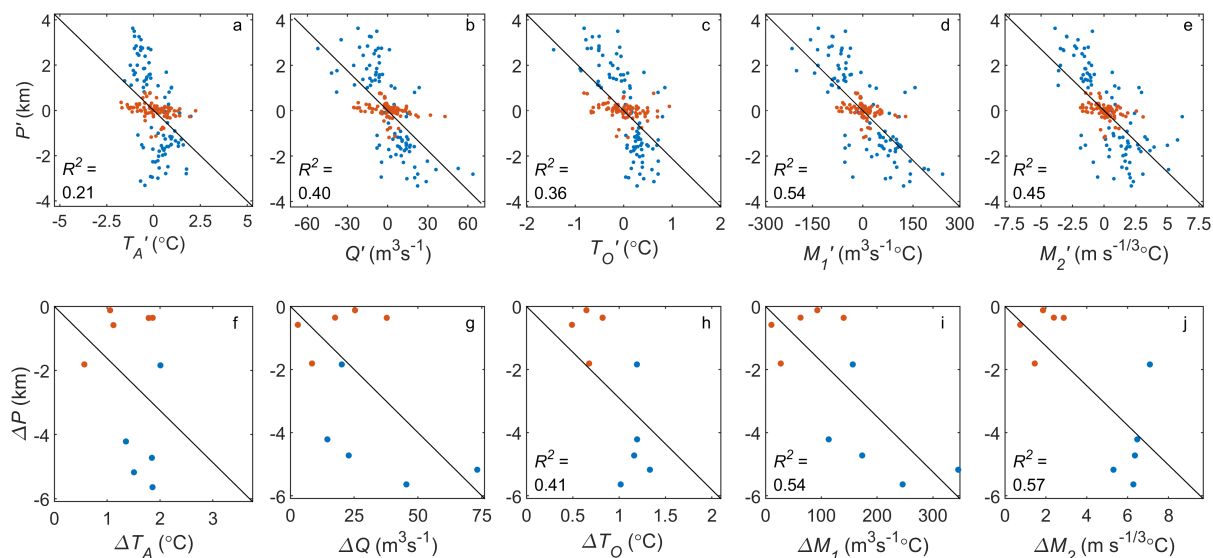
453

454 Figure 5. a-d. Relationship between anomalies in terminus position (P') and (a) air temperature (T_A')
455 (b) runoff (Q'), (c) ocean temperature (T_O'), and ocean/atmosphere forcing (d) M_1' and (e) M_2'.
456 Anomalies are shown relative to the 20-year mean at each glacier. f-j. Relationship between overall
457 change in terminus position (ΔP) and (f) air temperature (ΔT_A), (g) runoff (ΔQ), (h) ocean
458 temperature (ΔT), and ocean/atmosphere forcing (i) ΔM_1 and (j) ΔM_2. In each case, the overall
459 change is calculated by subtracting the mean 1993-1995 value from the mean 2010-2012 value. On
460 all plots, blue and red markers denote data from the southern and northern glaciers subsets
461 respectively, and black lines show the best fit to all data. R^2 values (all significant at $p < 0.05$) are
462 shown on all plots except (f) and (g), which are not significant at this level. Statistical values are given
463 in Table S3.

464
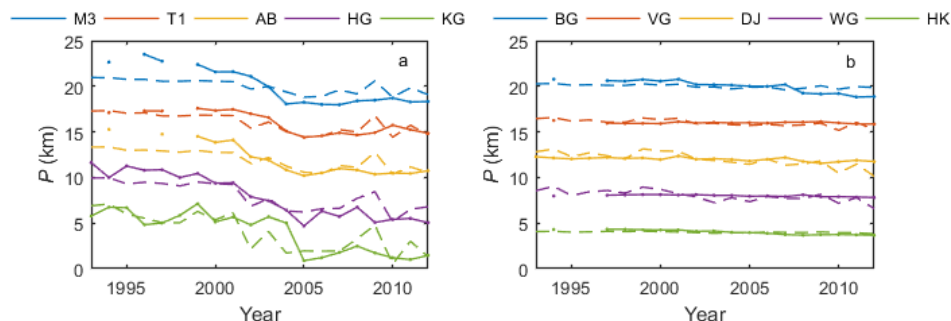
465

466 Figure 6. Change in terminus position P at the (a) southern glaciers and (b) northern glaciers, as
467 observed (solid lines) and parameterised based on equation (1) (dashed lines). P is shown relative to
468 an arbitrary up-glacier location, as in Figure 2e-f.

469

References

Aschwanden, A., Fahnestock, M. A. and Truffer, M. (2016) 'Complex Greenland outlet glacier flow captured', *Nature communications,* 7, pp. 10524.

Azetsu-Scott, K. and Syvitski, J. P. M. (1999) 'Influence of melting icebergs on distribution, characteristics and transport of marine particles in an East Greenland fjord', *Journal of Geophysical Research-Oceans,* 104(C3), pp. 5321-5328.

Bamber, J. L., Griggs, J. A., Hurkmans, R. T. W. L., Dowdeswell, J. A., Gogineni, S. P., Howat, I., Mouginot, J., Paden, J., Palmer, S., Rignot, E. and Steinhage, D. (2013) 'A new bed elevation dataset for Greenland', *Cryosphere,* 7(2), pp. 499-510.

Bartholomaus, T. C., Larsen, C. F. and O'Neel, S. (2013) 'Does calving matter? Evidence for significant submarine melt', *Earth and Planetary Science Letters,* 380, pp. 21-30.

Beenstock, M., Reingewertz, Y. and Paldor, N. (2012) 'Polynomial cointegration tests of anthropogenic impact on global warming', *Earth System Dynamics,* 3(2), pp. 173-188.

Benn, D. I., Cowton, T., Todd, J. and Luckman, A. (2017) 'Glacier calving in Greenland', *Current Climate Change Reports*, pp. 1-9.

Bevan, S. L., Luckman, A. J. and Murray, T. (2012) 'Glacier dynamics over the last quarter of a century at Helheim, Kangerdlugssuaq and 14 other major Greenland outlet glaciers', *Cryosphere,* 6(5), pp. 923-937.

Carr, J. R., Vieli, A. and Stokes, C. (2013) 'Influence of sea ice decline, atmospheric warming, and glacier width on marine-terminating outlet glacier behavior in northwest Greenland at seasonal to interannual timescales', *Journal of Geophysical Research-Earth Surface,* 118(3), pp. 1210-1226.

Carroll, D., Sutherland, D. A., Shroyer, E. L., Nash, J. D., Catania, G. A. and Stearns, L. A. (2017) 'Subglacial discharge-driven renewal of tidewater glacier fjords', *Journal of Geophysical Research: Oceans*.

Chauché, N., Hubbard, A., Gascard, J. C., Box, J. E., Bates, R., Koppes, M., Sole, A., Christoffersen, P. and Patton, H. (2014) 'Ice-ocean interaction and calving front morphology at two west Greenland tidewater outlet glaciers', *Cryosphere,* 8(4), pp. 1457-1468.

Christoffersen, P., O'Leary, M., Van Angelen, J. H. and van den Broeke, M. (2012) 'Partitioning effects from ocean and atmosphere on the calving stability of Kangerdlugssuaq Glacier, East Greenland', *Annals of Glaciology,* 53(60), pp. 249-256.

Cook, A., Holland, P., Meredith, M., Murray, T., Luckman, A. and Vaughan, D. (2016) 'Ocean forcing of glacier retreat in the western Antarctic Peninsula', *Science,* 353(6296), pp. 283-286.

Cowton, T., Sole, A., Nienow, P., Slater, D., Wilton, D. and Hanna, E. (2016) 'Controls on the transport of oceanic heat to Kangerdlugssuaq Glacier, east Greenland', *Journal of Glaciology*.

Dee, D. P., Uppala, S., Simmons, A., Berrisford, P., Poli, P., Kobayashi, S., Andrae, U., Balmaseda, M., Balsamo, G. and Bauer, d. P. (2011) 'The ERA-Interim reanalysis: Configuration and performance of the data assimilation system', *Quarterly Journal of the royal meteorological society,* 137(656), pp. 553-597.

Dowdeswell, J. (2004) *Cruise report - JR106b. RSS James Clark Ross. NERC Autosub Under Ice thematic programme. Kangerdlugssuaq Fjord and shelf, east Greenland*.

Engle, R. F. and Granger, C. W. J. (1987) 'Cointegration and error correction - representation, estimation and testing', *Econometrica,* 55(2), pp. 251-276.

Fenty, I., Willis, J. K., Khazendar, A., Dinardo, S., Forsberg, R., Fukumori, I., Holland, D., Jakobsson, M., Moller, D. and Morison, J. (2016) 'Oceans Melting Greenland: Early Results from NASA's Ocean-Ice Mission in Greenland', *Oceanography*.

Ferry, N., Parent, L., Garric, G., Drevillon, M., Desportes, C., Bricaud, C. and Hernandez, F. (2012) *Scientific Validation Report (ScVR) for Reprocessed Analysis and Reanalysis. MyOcean project report, MYO-WP04-ScCV-rea-MERCATOR-V1.0*.

Fried, M. J., Catania, G. A., Bartholomaus, T. C., Duncan, D., Davis, M., Stearns, L. A., Nash, J., Shroyer, E. and Sutherland, D. (2015) 'Distributed subglacial discharge drives significant

521   submarine melt at a Greenland tidewater glacier', *Geophysical Research Letters,* 42(21), pp.
522   1944-8007.
523 Fürst, J., Goelzer, H. and Huybrechts, P. (2015) 'Ice-dynamic projections of the Greenland ice sheet in
524   response to atmospheric and oceanic warming', *The Cryosphere,* 9(3), pp. 1039-1062.
525 Goelzer, H., Huybrechts, P., Fürst, J. J., Nick, F., Andersen, M. L., Edwards, T. L., Fettweis, X., Payne, A.
526   J. and Shannon, S. (2013) 'Sensitivity of Greenland ice sheet projections to model
527   formulations', *Journal of Glaciology,* 59(216), pp. 733-749.
528 Granger, C. W. and Newbold, P. (1974) 'Spurious regressions in econometrics', *Journal of*
529   *econometrics,* 2(2), pp. 111-120.
530 Holfort, J., Hansen, E., Østerhus, S., Dye, S., Jonsson, S., Meincke, J., Mortensen, J. and Meredith, M.
531   (2008) 'Freshwater fluxes east of Greenland', *Arctic-Subarctic Ocean Fluxes Defining the Role*
532   *of the Northern Seas in Climate.,* 304.
533 Howat, I. M., Joughin, I., Fahnestock, M., Smith, B. E. and Scambos, T. A. (2008) 'Synchronous retreat
534   and acceleration of southeast Greenland outlet glaciers 2000-06: ice dynamics and coupling
535   to climate', *Journal of Glaciology,* 54(187), pp. 646-660.
536 Inall, M. E., Murray, T., Cottier, F. R., Scharrer, K., Boyd, T. J., Heywood, K. J. and Bevan, S. L. (2014)
537   'Oceanic heat delivery via Kangerdlugssuaq Fjord to the south-east Greenland ice sheet',
538   *Journal of Geophysical Research: Oceans*, 119(2), pp. 631-645. Available at:
539   http://onlinelibrary.wiley.com/doi/10.1002/2013JC009295/abstract (Accessed 01).
540 Jakobsson, M., Mayer, L., Coakley, B., Dowdeswell, J. A., Forbes, S., Fridman, B., Hodnesdal, H.,
541   Noormets, R., Pedersen, R. and Rebesco, M. (2012) 'The international bathymetric chart of
542   the Arctic Ocean (IBCAO) version 3.0', *Geophysical Research Letters,* 39(12).
543 James, T. D., Murray, T., Selmes, N., Scharrer, K. and O'Leary, M. (2014) 'Buoyant flexure and basal
544   crevassing in dynamic mass loss at Helheim Glacier', *Nature Geoscience,* 7(8), pp. 594-597.
545 Jenkins, A. (2011) 'Convection-Driven Melting near the Grounding Lines of Ice Shelves and Tidewater
546   Glaciers', *Journal of Physical Oceanography,* 41(12), pp. 2279-2294.
547 Joughin, I., Howat, I. M., Fahnestock, M., Smith, B., Krabill, W., Alley, R. B., Stern, H. and Truffer, M.
548   (2008) 'Continued evolution of Jakobshavn Isbrae following its rapid speedup', *Journal of*
549   *Geophysical Research: Earth Surface,* 113(F4).
550 Joughin, I., Smith, B. E. and Medley, B. (2014) 'Marine Ice Sheet Collapse Potentially Under Way for
551   the Thwaites Glacier Basin, West Antarctica', *Science,* 344(6185), pp. 735-738.
552 Kaufmann, R. K. and Stern, D. I. (2002) 'Cointegration analysis of hemispheric temperature relations',
553   *Journal of Geophysical Research-Atmospheres,* 107(D1-D2).
554 Lea, J. M., Mair, D. W. F. and Rea, B. R. (2014) 'Instruments and Methods Evaluation of existing and
555   new methods of tracking glacier terminus change', *Journal of Glaciology,* 60(220), pp. 323-
556   332.
557 Luckman, A., Benn, D. I., Cottier, F., Bevan, S., Nilsen, F. and Inall, M. (2015) 'Calving rates at
558   tidewater glaciers vary strongly with ocean temperature', *Nature Communications,* 6.
559 McFadden, E. M., Howat, I. M., Joughin, I., Smith, B. and Ahn, Y. (2011) 'Changes in the dynamics of
560   marine terminating outlet glaciers in west Greenland (2000-2009)', *Journal of Geophysical*
561   *Research-Earth Surface,* 116.
562 Mills, T. C. (2009) 'How robust is the long-run relationship between temperature and radiative
563   forcing?', *Climatic change,* 94(3-4), pp. 351.
564 Moon, T., Joughin, I. and Smith, B. (2015) 'Seasonal to multiyear variability of glacier surface velocity,
565   terminus position, and sea ice/ice mélange in northwest Greenland', *Journal of Geophysical*
566   *Research: Earth Surface,* 120(5), pp. 818-833.
567 Murray, T., Scharrer, K., James, T. D., Dye, S. R., Hanna, E., Booth, A. D., Selmes, N., Luckman, A.,
568   Hughes, A. L. C., Cook, S. and Huybrechts, P. (2010) 'Ocean regulation hypothesis for glacier
569   dynamics in southeast Greenland and implications for ice sheet mass changes', *Journal of*
570   *Geophysical Research-Earth Surface,* 115.

571 Murray, T., Scharrer, K., Selmes, N., Booth, A. D., James, T. D., Bevan, S. L., Bradley, J., Cook, S., Llana,
572   L. C., Drocourt, Y., Dyke, L., Goldsack, A., Hughes, A. L., Luckman, A. J. and McGovern, J.
573   (2015) 'Extensive retreat of Greenland tidewater glaciers, 2000-2010', *Arctic Antarctic and*
574   *Alpine Research,* 47(3), pp. 427-447.
575 Nick, F. M., Vieli, A., Andersen, M. L., Joughin, I., Payne, A., Edwards, T. L., Pattyn, F. and van de Wal,
576   R. S. W. (2013) 'Future sea-level rise from Greenland's main outlet glaciers in a warming
577   climate', *Nature,* 497(7448), pp. 235-238.
578 Rignot, E. and Kanagaratnam, P. (2006) 'Changes in the velocity structure of the Greenland ice
579   sheet', *Science,* 311(5763), pp. 986-990.
580 Rignot, E., Xu, Y., Menemenlis, D., Mouginot, J., Scheuchl, B., Li, X., Morlighem, M., Seroussi, H., van
581   den Broeke, M., Fenty, I., Cai, C., An, L. and de Fleurian, B. (2016) 'Modeling of ocean-
582   induced ice melt rates of five west Greenland glaciers over the past two decades',
583   *Geophysical Research Letters,* 43(12), pp. 6374-6382.
584 Seale, A., Christoffersen, P., Mugford, R. I. and O'Leary, M. (2011) 'Ocean forcing of the Greenland
585   Ice Sheet: Calving fronts and patterns of retreat identified by automatic satellite monitoring
586   of eastern outlet glaciers', *Journal of Geophysical Research-Earth Surface,* 116.
587 Shreve, R. L. (1972) 'Movement of water in glaciers', *Journal of Glaciology,* 11, pp. 205-214.
588 Slater, D., Goldberg, D., Nienow, P. and Cowton, T. (2016) 'Scalings for submarine melting at
589   tidewater glaciers from buoyant plume theory', *Journal of Physical Oceanography,* in press.
590 Slater, D. A., Nienow, P. W., Goldberg, D. N., Cowton, T. R. and Sole, A. J. (2017) 'A model for
591   tidewater glacier undercutting by submarine melting', *Geophysical Research Letters,* 44(5),
592   pp. 2360-2368.
593 Straneo, F., Hamilton, G. S., Stearns, L. A. and Sutherland, D. A. (2016) 'Connecting the Greenland Ice
594   Sheet and the Ocean: A case study of Helheim Glacier and Sermilik Fjord', *Oceanography,*
595   29(4), pp. 34-45.
596 Straneo, F. and Heimbach, P. (2013) 'North Atlantic warming and the retreat of Greenland's outlet
597   glaciers', *Nature,* 504(7478), pp. 36-43.
598 Straneo, F., Heimbach, P., Sergienko, O., Hamilton, G., Catania, G., Griffies, S., Hallberg, R., Jenkins,
599   A., Joughin, I., Motyka, R., Pfeffer, W. T., Price, S. F., Rignot, E., Scambos, T., Truffer, M. and
600   Vieli, A. (2013) 'Challenges to Understanding the Dynamic Response of Greenland's Marine
601   Terminating Glaciers to Oceanic and Atmospheric Forcing', *Bulletin of the American*
602   *Meteorological Society,* 94(8), pp. 1131-1144.
603 Straneo, F., Sutherland, D. A., Holland, D., Gladish, C., Hamilton, G. S., Johnson, H. L., Rignot, E., Xu,
604   Y. and Koppes, M. (2012) 'Characteristics of ocean waters reaching Greenland's glaciers',
605   *Annals of Glaciology,* 53(60), pp. 202-210.
606 Sugiyama, S., Skvarca, P., Naito, N., Enomoto, H., Tsutaki, S., Tone, K., Marinsek, S. and Aniya, M.
607   (2011) 'Ice speed of a calving glacier modulated by small fluctuations in basal water
608   pressure', *Nature Geoscience,* 4(9), pp. 597-600.
609 Todd, J. and Christoffersen, P. (2014) 'Are seasonal calving dynamics forced by buttressing from ice
610   melange or undercutting by melting? Outcomes from full-Stokes simulations of Store
611   Glacier, West Greenland', *Cryosphere,* 8(6), pp. 2353-2365.
612 Todd, J., Christoffersen, P., Zwinger, T., Råback, P., Chauché, N., Benn, D., Luckman, A., Ryan, J.,
613   Toberg, N. and Slater, D. (2018) 'A Full-Stokes 3-D Calving Model Applied to a Large
614   Greenlandic Glacier', *Journal of Geophysical Research: Earth Surface.*
615 Todd, J., Christoffersen, P., Zwinger, T., Råback, P., Chauché, N., Benn, D. I., Luckman, A., Ryan, J.,
616   Toberg, N., Slater, D. and Hubbard, A. (in press) 'A Full-Stokes 3D Calving Model applied to a
617   large Greenlandic Glacier', *Journal of Geophysical Research: Earth Surface*.
618 van den Broeke, M., Box, J., Fettweis, X., Hanna, E., Noël, B., Tedesco, M., van As, D., van de Berg, W.
619   J. and van Kampenhout, L. (2017) 'Greenland Ice Sheet Surface Mass Loss: Recent
620   Developments in Observation and Modeling', *Current Climate Change Reports*, pp. 1-12.

621 Vieli, A., Jania, J. and Kolondra, L. (2002) 'The retreat of a tidewater glacier: observations and model
622   calculations on Hansbreen, Spitsbergen', *Journal of Glaciology,* 48(163), pp. 592-600.
623 Walsh, K., Howat, I., Ahn, Y. and Enderlin, E. (2012) 'Changes in the marine-terminating glaciers of
624   central east Greenland, 2000–2010', *The Cryosphere,* 6(1), pp. 211-220.
625 Wilson, N., Straneo, F. and Heimbach, P. (2017) 'Satellite-derived submarine melt rates and mass
626   balance (2011–2015) for Greenland's largest remaining ice tongues', *The Cryosphere,* 11(6),
627   pp. 2773-2782.
628 Wilson, N. J. and Straneo, F. (2015) 'Water exchange between the continental shelf and the cavity
629   beneath Nioghalvfjerdsbrae (79 North Glacier)', *Geophysical Research Letters,* 42(18), pp.
630   7648-7654.
631 Wilton, D. J., Jowett, A. M. Y., Hanna, E., Bigg, G. R., Van Den Broeke, M. R., Fettweis, X. and
632   Huybrechts, P. (2017) 'High resolution (1 km) positive degree-day modelling of Greenland ice
633   sheet surface mass balance, 1870–2012 using reanalysis data', *Journal of Glaciology,*
634   63(237), pp. 176-193.
635 Xu, Y., Rignot, E., Fenty, I., Menemenlis, D. and Flexas, M. M. (2013) 'Subaqueous melting of Store
636   Glacier, west Greenland from three-dimensional, high-resolution numerical modeling and
637   ocean observations', *Geophysical Research Letters,* 40(17), pp. 4648-4653.

638

639